

NUMERICAL SOLUTION OF THE SUPERSONIC LAMINAR FLOW OVER A TWO-DIMENSIONAL COMPRESSION CORNER USING AN IMPLICIT APPROACH

N. S. MADHAVAN AND V. SWAMINATHAN

Applied Mathematics Division, Vikram Sarabhai Space Centre, Trivandrum 695 022, India

SUMMARY

The use of an implicit numerical scheme, analogous to MacCormack's¹, for the supersonic laminar two-dimensional compression corner flow problem using unsteady Navier–Stokes equations is demonstrated. The technique entails a reduction of about 70 per cent in the computation time for a Courant number of 5, but it is characterized by an increase of approximately 20 per cent in computer memory requirement.

KEY WORDS Navier–Stokes Equations Compression Corner Flows Implicit Numerical Scheme Co-ordinate Transformation

INTRODUCTION

Explicit numerical schemes^{2,3} have been extensively used in the literature for the solution of two-dimensional unsteady Navier–Stokes equations in the context of compression corner flow problems. A major disadvantage of this technique is the long computation time, owing to the stringent limitation on the time step size. In the present paper, an implicit numerical method, analogous to that of MacCormack,^{1,4} has been successfully applied to solve the Navier–Stokes equations for the compression corner flow, transformed into a rectangular computational domain. The features of the flow field under investigation are depicted in Figure 1.

MATHEMATICAL FORMULATION

The unsteady two-dimensional Navier–Stokes equations may be written with respect to Cartesian co-ordinates in conservation form as

$$\frac{\partial \mathbf{U}}{\partial t} + \frac{\partial \mathbf{F}}{\partial x} + \frac{\partial \mathbf{G}}{\partial y} = \mathbf{0}, \quad (1)$$

where

$$\mathbf{U} = \begin{bmatrix} \rho \\ \rho u \\ \rho v \\ e \end{bmatrix},$$

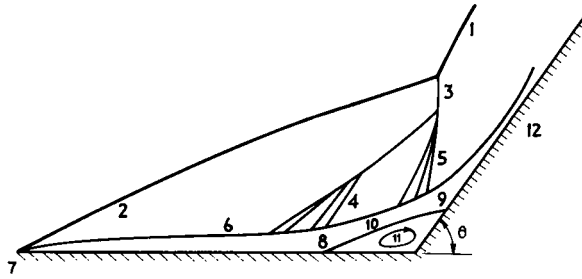


Figure 1. Schematic diagram of a supersonic flow field over a compression corner: (1) resultant shock; (2) leading edge shock; (3) induced shock; (4) separation compression fan; (5) reattachment compression fan; (6) boundary layer edge; (7) leading edge; (8) separation point; (9) reattachment point; (10) dividing streamline; (11) recirculating streamline; (12) neck region

$$\mathbf{F} = \begin{bmatrix} \rho u \\ \rho u^2 + \sigma_x \\ \rho uv + \tau_{xy} \\ (e + \sigma_x)u + \tau_{yx}v - k \frac{\partial T}{\partial x} \end{bmatrix},$$

$$\mathbf{G} = \begin{bmatrix} \rho v \\ \rho vu + \tau_{yx} \\ \rho v^2 + \sigma_y \\ (e + \sigma_y)v + \tau_{xy}u - k \frac{\partial T}{\partial y} \end{bmatrix},$$

$$\sigma_x = p - \lambda \left(\frac{\partial u}{\partial x} + \frac{\partial v}{\partial y} \right) - 2\mu \frac{\partial u}{\partial x},$$

$$\sigma_y = p - \lambda \left(\frac{\partial u}{\partial x} + \frac{\partial v}{\partial y} \right) - 2\mu \frac{\partial v}{\partial y},$$

$$\tau_{xy} = \tau_{yx} = -\mu \left(\frac{\partial u}{\partial y} + \frac{\partial v}{\partial x} \right),$$

the symbols having the same meanings as in Reference 1. Defining α such that $\alpha = 0$ upstream of the corner, and $\alpha = \theta$ downstream, the transformation $\xi = x$ and $\eta = y - (x - \text{RL}) \tan \alpha$, where RL is the distance from the leading edge to the corner, results in a computational domain which can be discretized into rectangular grids. Equation (1), when transformed into the new computational space, assumes the form

$$\frac{\partial \mathbf{U}'}{\partial t} + \frac{\partial \mathbf{F}'}{\partial \xi} + \frac{\partial \mathbf{G}'}{\partial \eta} = 0, \quad (2)$$

where

$$\mathbf{U}' = \mathbf{U}, \quad \mathbf{F}' = \mathbf{F}, \quad \mathbf{G}' = \mathbf{G} - \mathbf{F} \tan \alpha. \quad (3)$$

Differentiating equation (2) partially with respect to t , we obtain

$$\frac{\partial}{\partial t} \left(\frac{\partial \mathbf{U}}{\partial t} \right) = -\frac{\partial}{\partial \xi} \left(\mathbf{A} \frac{\partial \mathbf{U}}{\partial t} \right) - \frac{\partial}{\partial \eta} \left(\mathbf{B} \frac{\partial \mathbf{U}}{\partial t} \right), \quad (4)$$

where \mathbf{A} and \mathbf{B} are, respectively, the Jacobians of \mathbf{F}' and \mathbf{G}' w.r.t. \mathbf{U} . Implicitly approximating equation (4) and following Reference 1, we obtain

$$\left(\mathbf{I} + \Delta t \frac{\partial}{\partial \xi} \mathbf{A} \cdot + \Delta t \frac{\partial}{\partial \eta} \mathbf{B} \cdot \right) \delta \mathbf{U}_{ij}^{n+1} = \Delta \mathbf{U}_{ij}^n, \quad (5)$$

where

$$\delta \mathbf{U}_{ij}^{n+1} = \frac{\partial \mathbf{U}^{n+1}}{\partial t} \Delta t \quad \text{and} \quad \Delta \mathbf{U}_{ij}^n = \frac{\partial \mathbf{U}^n}{\partial t} \Delta t. \quad (6)$$

Now an implicit predictor–corrector scheme may be defined for the numerical integration of the transformed equations as follows:

Predictor

$$\begin{aligned} \Delta \mathbf{U}_{ij}^n &= -\Delta t \left(\frac{D_+}{\Delta \xi} \mathbf{F}'_{ij}{}^n + \frac{D_+}{\Delta \eta} \mathbf{G}'_{ij}{}^n \right), \\ \left(\mathbf{I} - \Delta t \frac{D_+}{\Delta \xi} |\mathbf{A}| \cdot \right) \left(\mathbf{I} - \Delta t \frac{D_+}{\Delta \eta} |\mathbf{B}| \cdot \right) \delta \mathbf{U}_{ij}^{n+1} &= \Delta \mathbf{U}_{ij}^n, \\ \mathbf{U}_{ij}^{n+1} &= \mathbf{U}_{ij}^n + \delta \mathbf{U}_{ij}^{n+1}. \end{aligned}$$

Corrector

$$\begin{aligned} \Delta \mathbf{U}_{ij}^{n+1} &= -\Delta t \left(\frac{D_-}{\Delta \xi} \mathbf{F}'_{ij}{}^{n+1} + \frac{D_-}{\Delta \eta} \mathbf{G}'_{ij}{}^{n+1} \right), \\ \left(\mathbf{I} + \Delta t \frac{D_-}{\Delta \xi} |\mathbf{A}| \cdot \right) \left(\mathbf{I} + \Delta t \frac{D_-}{\Delta \eta} |\mathbf{B}| \cdot \right) \delta \mathbf{U}_{ij}^{n+1} &= \Delta \mathbf{U}_{ij}^{n+1}, \\ \mathbf{U}_{ij}^{n+1} &= \frac{1}{2} [\mathbf{U}_{ij}^n + \mathbf{U}_{ij}^{n+1} + \delta \mathbf{U}_{ij}^{n+1}], \end{aligned} \quad (7)$$

where D_+ and D_- represent, respectively, forward and backward spatial difference operators, and dots indicate that the derivatives operate on all the factors to the right.

The matrices $|\mathbf{A}|$ and $|\mathbf{B}|$ have positive eigenvalues and are related to the Jacobians \mathbf{A} and \mathbf{B} . Let \mathbf{S}_ξ and \mathbf{S}_η and their inverses denote the matrices that diagonalize \mathbf{A} and \mathbf{B} , with $\mu = \lambda = k = 0$. Then, with perfect gas relations, \mathbf{A} and \mathbf{B} may be arranged as

$$\mathbf{A} = \mathbf{S}_\xi^{-1} \Lambda_A \mathbf{S}_\xi \quad (8)$$

and

$$\mathbf{B} = \mathbf{S}_\eta^{-1} \Lambda_B \mathbf{S}_\eta,$$

where

$$\mathbf{S}_\xi = \begin{bmatrix} 1 - \frac{\alpha\beta}{c^2} & \frac{u\beta}{c^2} & \frac{v\beta}{c^2} & -\frac{\beta}{c^2} \\ -uc + \alpha\beta & c - u\beta & -v\beta & \beta \\ -\frac{v}{\rho} & 0 & \frac{1}{\rho} & 0 \\ uc + \alpha\beta & -c - u\beta & -v\beta & \beta \end{bmatrix}, \quad (9)$$

$$\mathbf{S}_\eta = \begin{bmatrix} 1 - \frac{\alpha\beta}{c^2} & \frac{u\beta}{c^2} & \frac{v\beta}{c^2} & -\frac{\beta}{c^2} \\ \frac{\eta_x v - \eta_y u}{\rho\alpha_2} & \frac{\eta_y}{\rho\alpha_2} & \frac{-\eta_x}{\rho\alpha_2} & 0 \\ \beta_1 \left(\alpha\beta - c \frac{\alpha_1}{\alpha_2} \right) & \beta_1 \left(\frac{\eta_x}{\alpha_2} c - u\beta \right) & \beta_1 \left(\frac{\eta_y}{\alpha_2} c - u\beta \right) & \beta_1 \beta \\ \beta_1 \left(\alpha\beta + c \frac{\alpha_1}{\alpha_2} \right) & -\beta_1 \left(\frac{\eta_x}{\alpha_2} c + u\beta \right) & -\beta_1 \left(\frac{\eta_y}{\alpha_2} c + u\beta \right) & \beta_1 \beta \end{bmatrix}, \quad (10)$$

$$\alpha_1 = \eta_x u + \eta_y v, \quad \alpha_2 = (\eta_x^2 + \eta_y^2)^{1/2},$$

$$\alpha = \frac{1}{2}(u^2 + v^2), \quad \beta = \gamma - 1, \quad \beta_1 = 1/\sqrt{2}\rho c, \quad (11)$$

and Λ_A and Λ_B are diagonal matrices with the eigenvalues $(u, u + c, u, u - c)$ and $(\alpha_1, \alpha_1, \alpha_1 + c\alpha_2, \alpha_1 - c\alpha_2)$, respectively, as elements. The matrices $|\mathbf{A}|$ and $|\mathbf{B}|$ are defined by

$$|\mathbf{A}| = \mathbf{S}_\xi^{-1} \mathbf{D}_A \mathbf{S}_\xi \quad \text{and} \quad |\mathbf{B}| = \mathbf{S}_\eta^{-1} \mathbf{D}_B \mathbf{S}_\eta, \quad (12)$$

where \mathbf{D}_A and \mathbf{D}_B are, again, diagonal matrices with elements $(\lambda_{A_1}, \lambda_{A_2}, \lambda_{A_3}, \lambda_{A_4})$ and $(\lambda_{B_1}, \lambda_{B_2}, \lambda_{B_3}, \lambda_{B_4})$, respectively. Here,

$$\lambda_{A_1} = \max \left\{ |u| + \frac{2v}{\rho\Delta\xi} - \frac{1}{2} \frac{\Delta\xi}{\Delta t}, 0 \right\},$$

$$\lambda_{B_1} = \max \left\{ |\alpha_1| + \frac{2v}{\rho\Delta\eta} - \frac{1}{2} \frac{\Delta\eta}{\Delta t}, 0 \right\}, \quad (13)$$

with similar expressions for the other elements of the matrices \mathbf{D}_A and \mathbf{D}_B with $|u|$ and $|\alpha_1|$ replaced, respectively, by the absolute value of the corresponding eigenvalue, and

$$v = \max \left\{ \mu, \lambda + 2\mu, \frac{\gamma\mu}{Pr} \right\}.$$

It is easy to observe from equation (13) that for regions of the flow in which Δt satisfies the explicit stability criterion, all λ_{A_i} and λ_{B_i} vanish, and consequently the difference equations (7) just reduce to those of the explicit method.

COMPUTER PROGRAM AND RESULTS

A computer program was developed in FORTRAN for carrying out two-dimensional compression corner flow calculations and was made operational on the CDC CYBER 170/730 computer of Vikram Sarabhai Space Centre, Trivandrum. Thirty-two mesh points were used in the ξ -direction with the ramp at the 18th mesh point and the leading edge at the 4th. In the η -direction, a two-mesh system of a fine stretched mesh (of 18 points) near the wall and a coarse uniform mesh (of 10 points) away from the wall was employed.

The results obtained through the program for the following two specific cases for which literature values are readily available are now considered:

- (i) $M_\infty = 3.0$, $Re_L = 1.68 \times 10^4$, $\theta = 10^\circ$,
- (ii) $M_\infty = 4.0$, $Re_L = 6.8 \times 10^4$, $\theta = 10^\circ$.

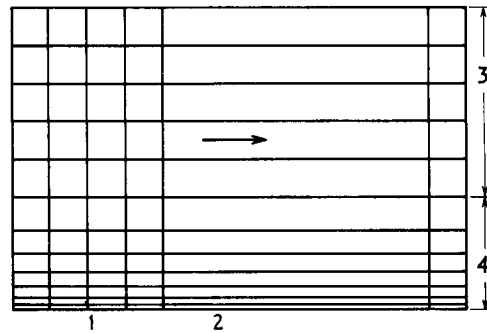


Figure 2. Computational domain after transformation: (1) leading edge; (2) compression corner; (3) uniform coarse mesh; (4) stretched fine mesh

Free-stream conditions were assumed (Figure 2) at the upstream and top mesh boundaries, while no slip condition at the wall and zero-order extrapolation at the downstream boundary were applied.

The data processing rate was about 3.4×10^{-3} s per grid point including prediction and correction, i.e. on an average, about 60 per cent more than that for the explicit scheme. Thus, when a CFL (Courant–Friedrichs–Lewy) number of 5 was used, the implicit scheme took about one-third of the time for the explicit method, yielding a speed-up factor of approximately 3. CFL numbers upto about 15 could be used in the specific examples without loss of accuracy. About 250 iterations were required to obtain convergence when the difference in the flow parameter values between two successive iterations became less than about 0.1 per cent, and this took about 11 min on the CDC computer.

It is also observed that for the implicit method, the memory requirement is marginally more, owing to the fact that the Δu s of all elements of the state vector for all mesh points need to be stored. Thus, for the 32×28 mesh system, although the explicit method requires about 2×10^4 60-bit words of memory, an additional 4×10^3 words will have to be available for the implicit case. In other words, the increase in memory requirement for the implicit scheme is of the order of 20 per cent.

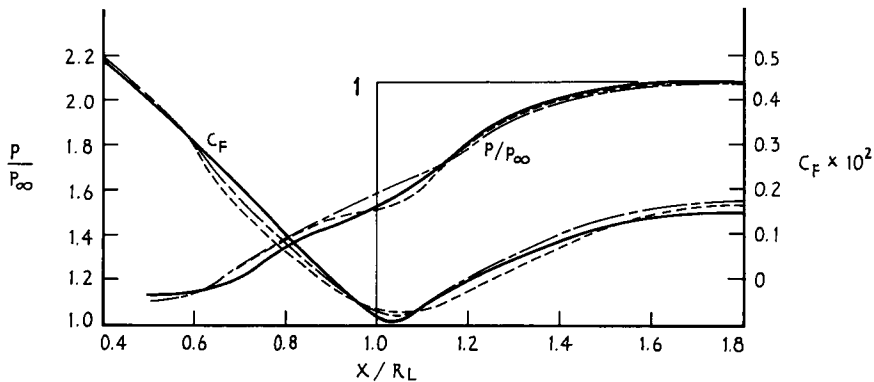


Figure 3. Comparison of wall pressure and skin friction ($M_\infty = 3.0$, $Re_L = 1.68 \times 10^4$, $\theta = 10^\circ$): results from implicit method; ——— Carter's results; ---- MacCormack's results. 1 indicates inviscid results

Figure 3 presents the surface pressure distribution and skin friction as obtained through the program for case (i). The corresponding computed values of Carter³ and MacCormack² are also shown in the Figure and the comparison is quite good. Figure 4 describes the surface pressure distribution and skin friction for the Mach 4 flow (case (ii)), which is again in reasonable conformity with the experimental surface pressure values due to Lewis⁶ as also Carter's computed values³ exhibited in the same figure.

Figure 5 presents a plot of the computation time to reach steady state against the Courant number used in the implicit numerical scheme for case (i), giving an idea of the speed-up factor as compared to the explicit numerical method.

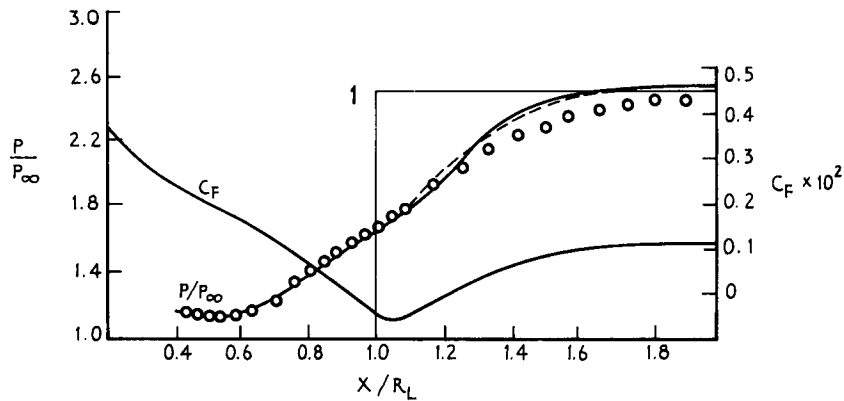


Figure 4. Comparison of wall pressure and skin friction ($M_\infty = 4.0$, $Re_L = 6.8 \times 10^4$, $\theta = 10^\circ$):—results from implicit method; $\circ \circ$ experimental results; - - - results from Carter, 1 indicates inviscid results

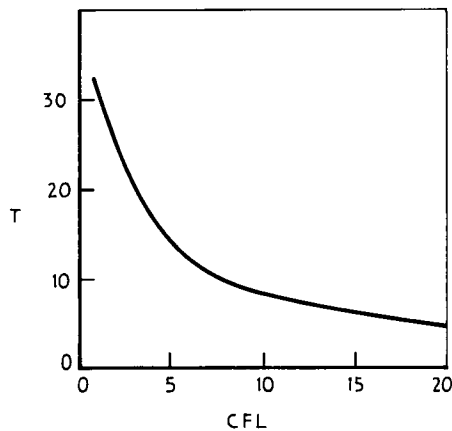


Figure 5. Computation time to reach steady state vs. Courant number used in the implicit scheme ($M_\infty = 3.0$, $Re_L = 1.68 \times 10^4$, $\theta = 10$, 32×28 mesh)

ACKNOWLEDGEMENT

The authors are grateful to the referee for valuable suggestions.

REFERENCES

1. R. W. MacCormack, 'A numerical method for solving the equations of compressible viscous flow', *AIAA Journal*, **20**, (9), 1275–1281 (1982).
2. C. M. Hung and R. W. MacCormack, 'Numerical solution of supersonic and hypersonic laminar compression corner flows', *AIAA Journal*, **14**, 475–481 (1976).
3. J. E. Carter, 'Numerical solutions of the Navier–Stokes equations for the supersonic laminar flow over a two-dimensional compression corner', *NASA Report TR R-385*, 1972.
4. V. Swaminathan and N. S. Madhavan, 'Computer solutions of Navier–Stokes equations for shock wave–turbulent boundary layer interactions far away from the leading edge', in C. Taylor, J. A. Johnson and W. R. Smith (eds), *Numerical Methods in Laminar and Turbulent Flow, Proc. Third International Conference*, University of Washington, Seattle, 8–11 August, 1983, Pineridge Press, Swansea, 1983, Paper No. 21, pp. 221–231.
5. S. L. Lawrence, J. C. Tannehill and D. S. Chaussee, 'Application of the implicit MacCormack scheme to the parabolized Navier–Stokes equations', *AIAA Journal*, **22**, (12), 1755–1763 (1984).
6. J. E. Lewis, T. Kubota and L. Lees, 'Experimental investigation of supersonic laminar two-dimensional boundary layer separation in a compression corner with and without cooling', *AIAA Journal*, **8**, (1), 7–14 (1968).